Interplay between R 4f and Fe 3d states in charge-ordered RFe$_2$O$_4$ (R = Er, Tm, Lu)

D. H. Kim,[1] Jihoon Hwang,[1] Eunsook Lee,[1] J. Kim,[2] B. W. Lee,[2] Han-Koo Lee,[3] J.-Y. Kim,[3] S. W. Han,[4] S. C. Hong,[4] Chang-Jong Kang,[5] B. I. Min,[5] and J.-S. Kang[1,*]

[1]*Department of Physics, The Catholic University of Korea, Bucheon 420-743, Korea*
[2]*Department of Physics, Hankuk University of Foreign Studies, Yongin 449-791, Korea*
[3]*Pohang Accelerator Laboratory (PAL), POSTECH, Pohang 790-784, Korea*
[4]*Department of Physics and Energy Harvest-Storage Research Center, University of Ulsan, Ulsan 680-749, Korea*
[5]*Department of Physics, POSTECH, Pohang 790-784, Korea*

(Received 29 November 2012; revised manuscript received 10 February 2013; published 10 May 2013)

The electronic structures of R 4f and Fe 3d states of RFe$_2$O$_4$ (R = Er, Tm, Lu) have been investigated by employing soft x-ray absorption spectroscopy (XAS) and magnetic circular dichroism at the Fe 2p and R 3d absorption edges. It is found that the valence states of Fe and R ions are nearly Fe$^{2.5+}$ and R^{3+}, and that the net magnetic moments of Fe^{2+} and Fe^{3+} ions are antiparallel to each other. Both R 3d and O 1s XAS spectra show that the localized R 4f states do not contribute to the multiferroicity of RFe$_2$O$_4$. On the other hand, the magnetization data for RFe$_2$O$_4$ at low temperature (T) reveal the cluster glass behavior for R = Tm and Lu, but not for R = Er. This work suggests that the T-dependent structural differences among RFe$_2$O$_4$, caused by different R ions, are closely related to the magnetoelectricity at low temperature.

DOI: 10.1103/PhysRevB.87.184409 PACS number(s): 75.85.+t, 78.20.Ls, 78.70.Dm, 75.50.Gg

I. INTRODUCTION

Multiferroicity that represents the coupled phenomenon between magnetism and ferroelectricity has attracted much attention due to potential technical applications as well as scientific interest. Multiferroic phenomena have been observed mostly in manganese oxides.[1] LuFe$_2$O$_4$ was reported to be the first iron (Fe) -based multiferroic system having a charge ordering (CO).[2] LuFe$_2$O$_4$ is a small energy-gap magnetic insulator,[3] possessing a large coercivity.[4,5] Even though the multiferroicity in LuFe$_2$O$_4$ is currently under debate as to whether it is an intrinsic property or not,[6–10] it has stimulated the investigation of magnetoelectricity in the RFe$_2$O$_4$ (where R denotes rare earth) family having other R elements.[11–14] But not much progress has been achieved yet. In particular, the role of R 4f electrons in determining the magnetoelectric properties of RFe$_2$O$_4$ with different R elements has not been explored.

RFe$_2$O$_4$ (R = Y, Ho, Er, Tm, Yb, Lu) crystallizes in the rhombohedral structure with the $R\bar{3}m$ space group at room temperature, which consists of the alternate stacking of the Fe-O and R-O triangular lattices (see Fig. 1).[15–18] Figure 1 shows the CO state of LuFe$_2$O$_4$, proposed by Yamada *et al.*,[16] in which equal amounts of the charge-ordered divalent Fe^{2+} and trivalent Fe^{3+} ions coexist, resulting in the average nominal valence states of Fe$^{2.5+}$. Due to its inherent nature of the geometrical frustration, the ground-state CO and the magnetic structure of LuFe$_2$O$_4$ have not been clearly resolved yet.[8,19,20] The magnetic properties of RFe$_2$O$_4$ are governed mainly by Fe ions, but their temperature (T) -dependent properties depend on R very much. The RFe$_2$O$_4$ family exhibits a ferrimagnetic transition at $T_C \sim 240$ K.[2,13,14] YFe$_2$O$_4$ and ErFe$_2$O$_4$ exhibit a two-step phase transition: a magnetic transition at $T_{C1} \sim 240$ K and a structural transition to the monoclinic phase at $T_{C2} \sim$ 190–200 K.[21,22] Recently, monoclinic distortion below T_C has also been indicated in LuFe$_2$O$_4$.[8] On the other hand, no clear structural transitions were observed in TmFe$_2$O$_4$ and YbFe$_2$O$_4$.[22]

The first step to understand the different magnetic and structural properties of RFe$_2$O$_4$ for different R elements would be to investigate the electronic structures of their Fe 3d and R 4f states. Soft x-ray absorption spectroscopy (XAS)[23,24] and soft x-ray magnetic circular dichroism (XMCD)[25,26] are powerful experimental tools for studying the valence and spin states of transition-metal (T) and rare-earth ions in solids and the element-specific local magnetic moments of spin and orbital components. In this work, we have investigated the electronic structures of Fe 3d and R 4f states in RFe$_2$O$_4$ (R = Er, Tm, Lu) by employing XAS and XMCD.

II. EXPERIMENTAL DETAILS

Polycrystalline RFe$_2$O$_4$ (R = Er, Tm, Lu) samples were synthesized by using solid-state reaction methods.[13,14] X-ray diffraction (XRD) measurements showed that these samples have a single-phase rhombohedral structure (space group $R\bar{3}m$). Magnetization measurements were done using a commercial vibrating sample magnetometer (Lake Shore, model 7300). The temperature (T) dependence of magnetization $M(T)$ was measured in both the zero-field-cooled (ZFC) and field-cooled (FC) modes, where the FC magnetization data were obtained while cooling the sample under a magnetic field.

XAS and XMCD experiments were performed at the 2A elliptically polarized undulator (EPU) beamline of the Pohang Light Source (PLS). Samples were cleaned *in situ* by repeated scraping with a diamond file. The chamber pressure was better than 3×10^{-10} Torr. XAS and XMCD spectra were obtained by using the total electron yield (TEY) mode, and XMCD spectra were obtained under a magnetic field of $H \sim 0.6$ T. XAS and XMCD spectra were obtained at 220, 200, and 170 K. Unfortunately, these samples showed a strong charging effect in the TEY mode, which prevented us from obtaining the intrinsic XMCD spectra at low temperatures across the structural and magnetic transitions. In this paper, we present

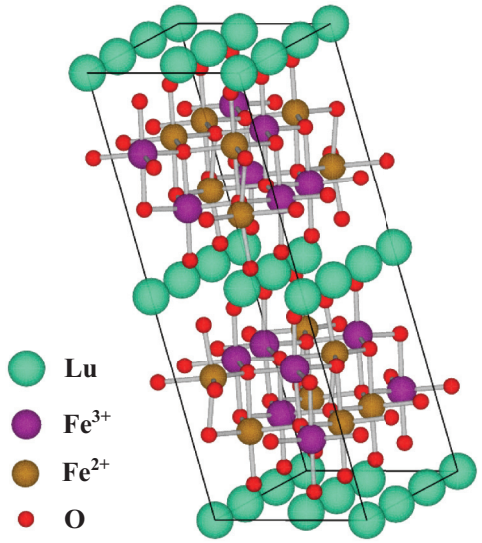

FIG. 1. (Color online) Crystal structure of $LuFe_2O_4$, which consists of the alternate stacking of the Fe-O and Lu-O triangular lattices along the c axis. Fe ions in Fe_2O_4 layers form the triangular lattices.

the XMCD spectra, obtained at $T \approx 220$ K only, a little below T_C.[27] The total resolution for XAS and XMCD was set at ~100 meV at $h\nu \sim 600$ eV. All the spectra were normalized to the incident photon flux.

III. RESULTS AND DISCUSSION

Figure 2 shows the ZFC and FC magnetization for $R\mathrm{Fe_2O_4}$ under the external field of $H = 1$ kOe. All three samples show the ferrimagnetic transition at $T_C \approx 240$ K, in agreement with those in other $R\mathrm{Fe_2O_4}$.[22,28,29] For $R =$ Tm and Lu, the larger magnetization is observed under field cooling, which is characteristic of a cluster glass system[30] and considered to originate from the growing size of the magnetic domains along $\vec{H}$. The cluster glass behavior in $R\mathrm{Fe_2O_4}$ is expected because of its generic nature of the geometrical and magnetic frustration.

Note that there are differences in $M(T)$ among $R =$ Er, Tm, Lu. First, the $M(T)$ data of $R =$ Er are distinctly different from those of $R =$ Tm and Lu, suggesting that the low-T state of $ErFe_2O_4$ is not a cluster glass state. Secondly, the FC magnetization of $R =$ Tm increases monotonically with decreasing T, in contrast with $R =$ Er and Lu. The FC curve of $R =$ Er exhibits two anomalies at $T_{C1} \approx 240$ and $T_{C2} \approx 210$ K. The second transition at T_{C2} arose from the structural transition to monoclinic phase.[22] In $R =$ Er, the ZFC magnetization is extraordinarily higher than the FC magnetization near $T_C \approx 240$ K.[31] This feature is expected to come from the hysteresis behavior accompanied by the structural transition, or reflects the very large magnetic anisotropy near T_C. The FC curve of $R =$ Lu shows a slight decrease below $T \approx 170$ K, which is also related to the structural distortion subsequent to the magnetic ordering.[3,8,12,32] The cluster glass behavior is retained for $LuFe_2O_4$ even below $T \approx 170$ K, whereas it disappears in the monoclinic phase of $ErFe_2O_4$. Therefore the different magnetic behaviors in $R\mathrm{Fe_2O_4}$ at low temperature,

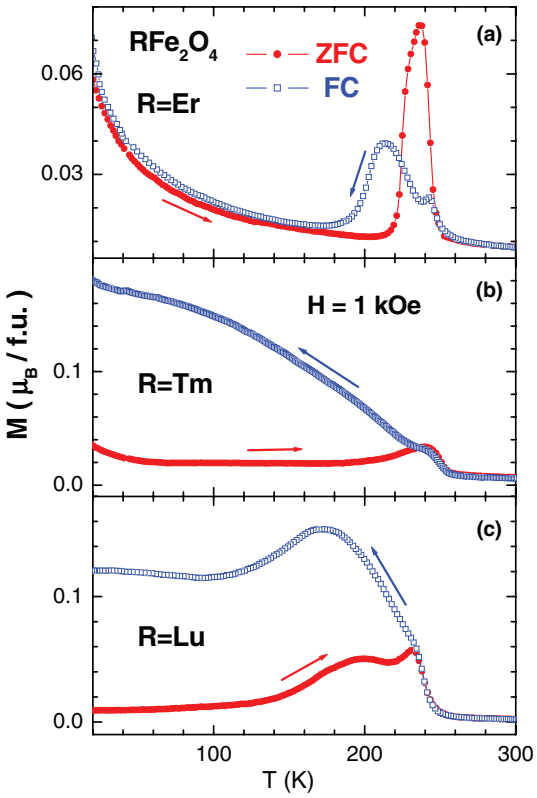

FIG. 2. (Color online) Temperature dependence of magnetization $M(T)$ for $R\mathrm{Fe_2O_4}$ ($R =$ Er, Tm, Lu), measured under an external field of $H = 1$ kOe. FC and ZFC denote field-cooled and zero-field-cooled magnetization, respectively.

shown in Fig. 2, suggest an intimate relationship between the structure and magnetism in $R\mathrm{Fe_2O_4}$.

Figure 3 shows the measured Fe $2p$ XAS spectra of $R\mathrm{Fe_2O_4}$ ($R =$ Er, Tm, Lu). L_3 ($2p_{3/2}$) and L_2 ($2p_{1/2}$) peaks arise from the spin-orbit coupling of the $2p$ core hole. This figure shows that the Fe $2p$ XAS spectra of $R\mathrm{Fe_2O_4}$ are essentially identical to one another for $R =$ Er, Tm, Lu, as shown more clearly in the inset. This finding indicates that the valence states of Fe ions are essentially the same for $R =$ Er, Tm, Lu. The spectral feature in the L_3 region is represented by the prominent two peaks corresponding to the Fe^{2+} and Fe^{3+} states, respectively. A comparison of the Fe $2p$ XAS of $R\mathrm{Fe_2O_4}$ with those of divalent FeO (Fe^{2+}) and trivalent α-Fe_2O_3 (Fe^{3+}) reference oxides shows that Fe ions are in the Fe^{2+}-Fe^{3+} mixed-valent states in all $R =$ Er, Tm, Lu. This finding agrees with the previous XAS studies of $LuFe_2O_4$.[8,33–35]

Figure 4(a) shows the two absorption spectra and the dichroism (XMCD) spectrum of $TmFe_2O_4$. To minimize the charging effect in these insulating samples, these spectra were obtained at $T \approx 220$ K,[27] a little below T_C (see Fig. 2), as described above. The two absorption spectra were obtained with the photon helicity parallel to (ρ_+, red curve) and antiparallel to (ρ_-, black curve) the applied magnetic field, respectively, and the XMCD spectrum (the bottom blue curve) was obtained by taking the difference between them ($\Delta\rho = \rho_+ - \rho_-$). This figure shows that the signs of the dichroism signals from divalent Fe^{2+} states and trivalent Fe^{3+} states are

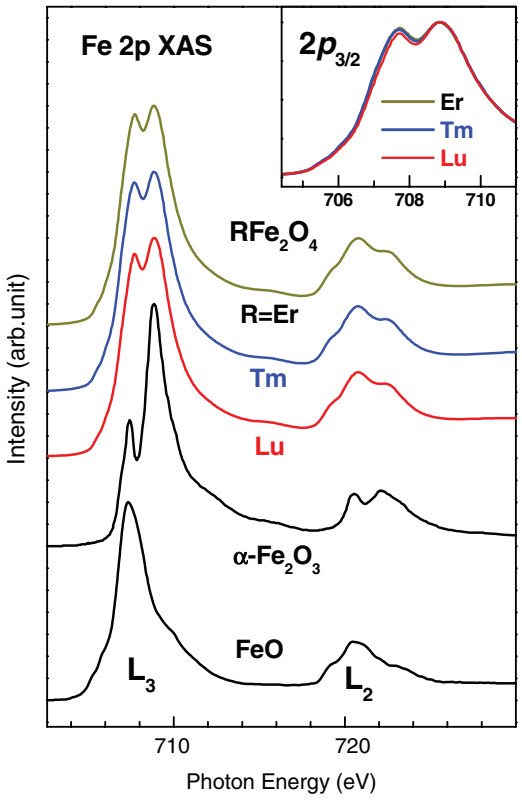

FIG. 3. (Color online) Fe $2p$ XAS spectra of $R\mathrm{Fe_2O_4}$ in comparison to those of reference Fe oxides. Inset: Comparison of the Fe $2p_{3/2}$ XAS part.

opposite to each other, in agreement with the findings in both single- and polycrystalline $\mathrm{LuFe_2O_4}$.[8,33–35]

Further, Fig. 4(b) shows that the line shapes of the Fe $2p$ XMCD spectra of $R\mathrm{Fe_2O_4}$ are very similar among $R =$ Er, Tm, Lu. As in $R =$ Tm [see Fig. 4(a)], in $R =$ Lu and Er the negative and positive L_3 XMCD signals come from Fe^{2+} and Fe^{3+}, respectively. The relatively weaker dichroic signals for Fe^{3+} than those for Fe^{2+} indicate the partial cancellation of the Fe^{3+} magnetic moments, implying that not all Fe^{3+} spins order parallel in $R\mathrm{Fe_2O_4}$, whereas most of the Fe^{2+} spins order parallel (see Fig. 7 below). In any case, Fig. 4 provides evidence that the net magnetic moments of Fe^{2+} and Fe^{3+} ions are antiparallel to each other in all of $R\mathrm{Fe_2O_4}$ ($R =$ Er, Tm, Lu), which supports their ferrimagnetic ground states.

This feature is different from that observed in Er-doped $\mathrm{Lu_{1-x}Er_xFe_2O_4}$.[35] In Ref. 35, the XMCD signals of Fe^{3+} almost vanished for $x = 0.5$ ($\mathrm{Lu_{0.5}Er_{0.5}Fe_2O_4}$), which was interpreted to indicate the disappearance of the long-range order of Fe^{3+} ions due to the site and structural disorder at R sites. In contrast, our XMCD data for $\mathrm{ErFe_2O_4}$ (corresponding to $x = 1$ in $\mathrm{Lu_{1-x}Er_xFe_2O_4}$ without having the structural and site disorder) are quite different. Such differences between $x = 0.5$ (Ref. 35) and $x = 1$ (this work) again indicate that the magnetism in $R\mathrm{Fe_2O_4}$ is closely related to its structure depending on R, as pointed out in Fig. 2.

Figures 5(a) and 5(b) show the $R\ 3d_{5/2}$ XAS spectra of $R\mathrm{Fe_2O_4}$ for $R =$ Er and Tm,[36] which are governed by the transition from the $R\ 3d_{5/2}$ core states to the unoccupied $R\,4f$ states. As a guide to the valence states of R ions, these spectra are compared to those of Er and Tm metals.[37] These $R\ 3d$ XAS spectra of $R\mathrm{Fe_2O_4}$, with $R =$ Er, Tm, are very similar to those of the corresponding rare-earth metals. It is well known that Er and Tm ions are trivalent in metals, having $4f^{11}$ and $4f^{12}$ configurations, respectively, in the ground states.[38,39] The

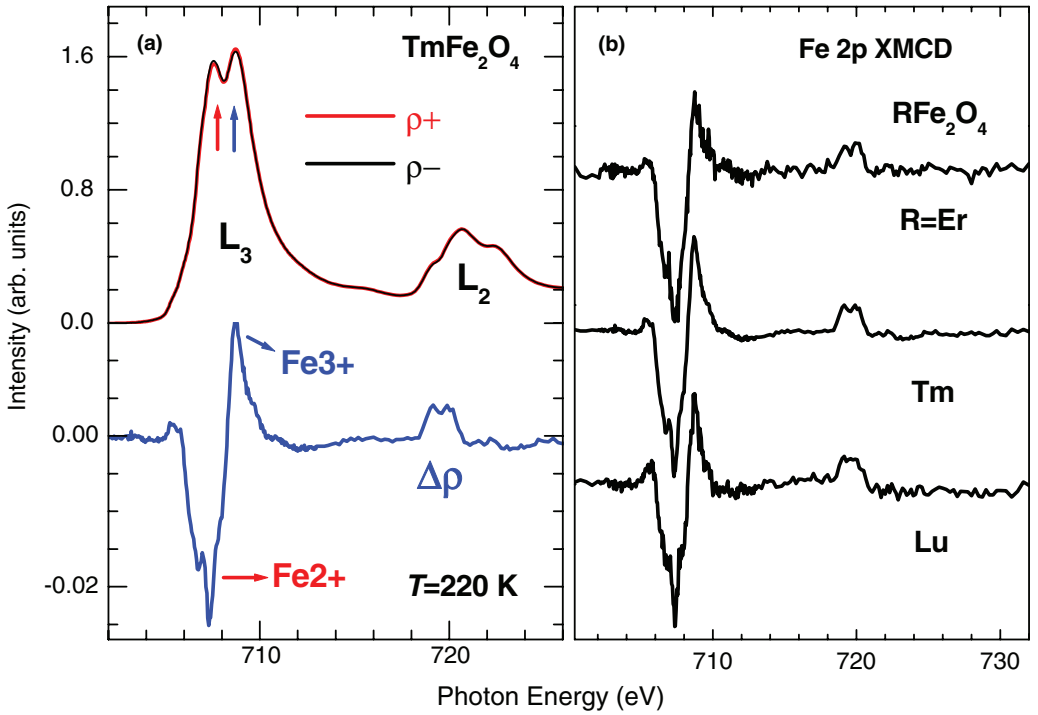

FIG. 4. (Color online) (a) Fe $2p$ absorption spectra of $\mathrm{TmFe_2O_4}$, obtained with different photon helicities, ρ_+ and ρ_-, and the XMCD spectrum, derived from $\Delta\rho = \rho_+ - \rho_-$. (b) Comparison of the Fe $2p$ MCD spectra of $R\mathrm{Fe_2O_4}$ ($R =$ Er, Tm, Lu).

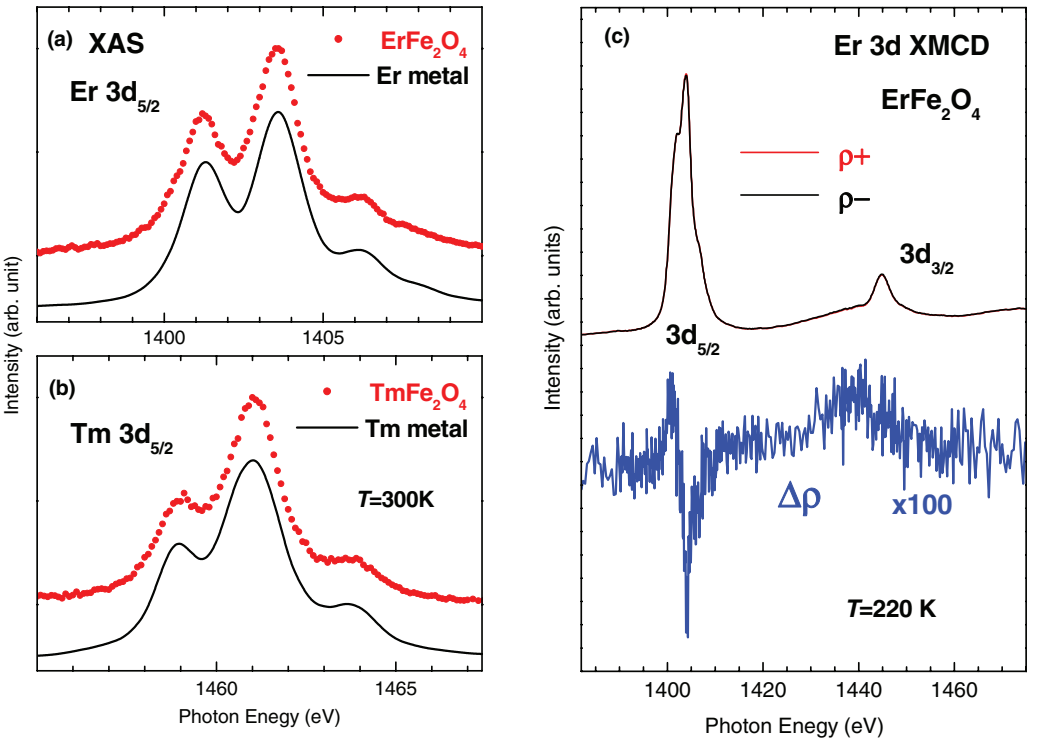

FIG. 5. (Color online) R $3d_{5/2}$ XAS (M_4 edge) spectra of $R\mathrm{Fe_2O_4}$ for (a) R = Er and (b) R = Tm. They are compared to those of Er and Tm metals, taken from Ref. 37, respectively. (c) Er $3d$ XMCD spectra of $\mathrm{ErFe_2O_4}$.

close similarity between the R $3d$ XAS spectra of insulating $R\mathrm{Fe_2O_4}$ oxides and R metals (R = Er, Tm) reflects the fact that the localized R $4f$ states are not sensitive to the crystal electric field (CEF) of the surrounding elements. This can be understood as follows: R $4f$ wave functions are located within the outer shells so that they are shielded well from the CEF. Hence the R $3d$ absorption spectra become similar irrespective of metals and oxides. Therefore, this figure provides evidence that R ions are trivalent and that R $4f$ electrons are very localized in $R\mathrm{Fe_2O_4}$ (R = Er, Tm, Lu).

Figure 5(c) shows the Er $3d$ XMCD spectra of $\mathrm{ErFe_2O_4}$. The sign of the Er $3d$ XMCD spectrum indicates that the magnetic moment of Er $4f$ states is parallel to that of Fe^{2+} states, but antiparallel to that of Fe^{3+} states (see Fig. 4). However, the dichroism signals of Er $3d$ states are very weak. The findings in Figs. 5(b) and 5(c) thus suggest that R $4f$ electrons do not contribute directly to the magnetoelectricity in $R\mathrm{Fe_2O_4}$ (R = Er, Tm, Lu).

Figure 6 shows that the O $1s$ XAS spectra of $R\mathrm{Fe_2O_4}$ (R = Er, Tm, Lu) are very similar to one another for different R elements. The O $1s$ XAS spectra of transition-metal oxides represent the unoccupied T $3d$ and $4s/4p$ states, as well as the other conduction-band states via the hybridization with the unoccupied O $2p$ states.[40] Then this finding indicates that the unoccupied R $4f$ states are not observed in the O $1s$ XAS spectra, reflecting the fact that the hybridization between R $4f$ and O $2p$ states is very weak. Therefore, we assign the peaks in O $1s$ XAS similarly to those in other transition-metal oxides without having R ions.[41] The peaks from the low energy are assigned to the unoccupied Fe $3d$ states of Fe^{3+} ions, Fe $3d$ states of Fe^{2+} ions, and R $5d$-Fe $4sp$ states, respectively. These assignments are supported by the calculated electronic structures shown in Fig. 7.[42]

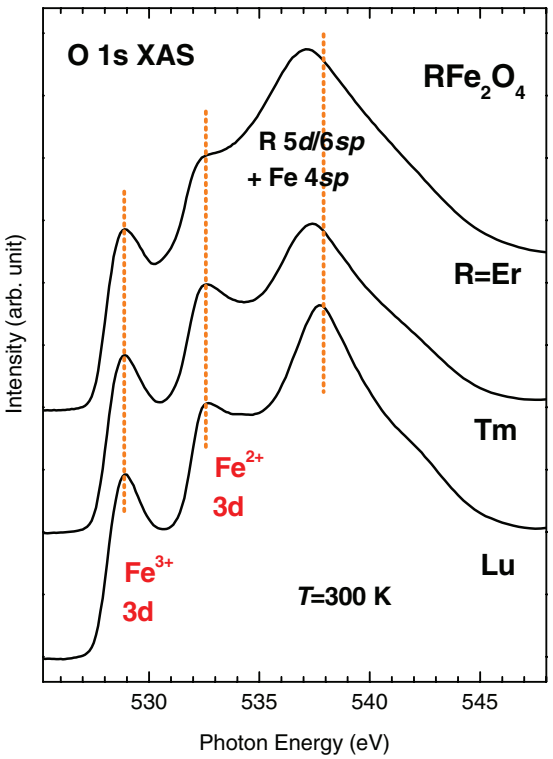

FIG. 6. (Color online) Comparison of the O $1s$ XAS spectra of $R\mathrm{Fe_2O_4}$ (R = Er, Tm,Lu).

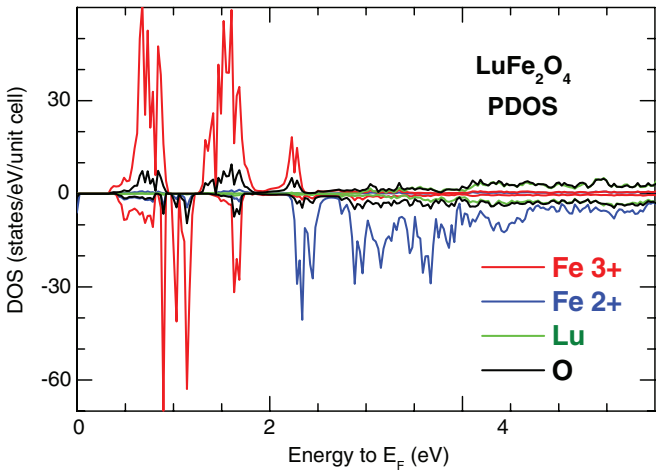

FIG. 7. (Color online) Unoccupied projected densities of states above E_F of $LuFe_2O_4$, obtained by using the DFT + SO + U band method.[42]

Figure 7 provides the calculated projected densities of states (PDOS's) of Fe^{3+}, Fe^{2+}, Lu, and O ions in $LuFe_2O_4$, which were obtained from the density functional theory (DFT) band calculations for the ferrimagnetic CO state of $LuFe_2O_4$.[16,19] In the DFT calculations, both the spin-orbit (SO) interaction and the Coulomb interaction U were incorporated (DFT + SO + U). As mentioned above, the net spins of Fe^{2+} and Fe^{3+} ions in $LuFe_2O_4$ are antiparallel. Note, however, that there are three types of Fe^{3+} ions in $LuFe_2O_4$. Two of them have the antiparallel spin configurations to Fe^{2+}, while the other one has the parallel spin configuration to Fe^{2+}.[35] That is why there are both spin-up and -down components of Fe^{3+} ions in Fig. 7. The unoccupied states near the Fermi level (E_F) are mainly Fe 3d states of Fe^{3+} ions, while Fe 3d states of Fe^{2+} ions are located far above E_F. These calculated PDOS's agree quite well with the measured O 1s XAS spectra in Fig. 6. The PDOS's for R = Er and Tm are expected to be similar to those of Lu, except for the R 4f PDOS. Note that there are no unoccupied Lu 4f states because Lu 4f states are almost filled.

IV. CONCLUSION

The valence and spin states of RFe_2O_4 (R = Er, Tm, Lu) have been investigated by performing XAS and XMCD measurements at the Fe 2p and R 3d absorption edges. The magnetization measurement for RFe_2O_4 reveal the cluster glass behavior for R = Tm and Lu, while it is not so clear for R = Er. The valence states of Fe and R ions are found to be nearly $Fe^{2.5+}$ and R^{3+}. The Fe 2p XMCD spectra, obtained at T = 220 K, provide evidence that the net magnetic moments of Fe^{2+} and Fe^{3+} ions are antiparallel to each other, in agreement with their ferrimagnetic ground states. The dichroism signals of Er 3d states, although very weak, show that the magnetic moments of the Er 4f states are parallel to those of Fe^{2+} ions. Both R 3d and O 1s XAS spectra indicate that the localized R 4f states are not sensitive to the crystal electric field, implying that they do not contribute directly to the magnetoelectricity of RFe_2O_4. On the other hand, the T-dependent structural differences among RFe_2O_4 for different R ions are closely related to their T-dependent magnetic properties, and so they are expected to affect the possible magnetoelectricity of RFe_2O_4 at low temperature.

ACKNOWLEDGMENTS

This work was supported by the NRF under Contracts No. 2011-0022444 and No. 2009-0079947. J.K. and B.W.L. acknowledge support by Grant No. NRF-2012R1A1A2008845. S.C.H. and S.W.H. acknowledge support by Grants No. NRF-2009-0093818 (Priority Research Centers Program) and No. NRF-2012-006888. Experiment at PLS was supported by MSIP and PAL, Korea.

*Author to whom all correspondence should be addressed: kangjs@catholic.ac.kr

[1]T. Kimura, T. Goto, H. Shintani, K. Ishizaka, T. Arima, and Y. Tokura, Nature (London) **426**, 55 (2003).
[2]N. Ikeda, H. Ohsumi, K. Ohwada, K. Ishii, T. Inami, K. Kakurai, Y. Murakami, K. Yoshii, S. Mori, Y. Horibe, and H. Kito, Nature (London) **436**, 1136 (2005).
[3]X. S. Xu, M. Angst, T. V. Brinzari, R. P. Hermann, J. L. Musfeldt, A. D. Christianson, D. Mandrus, B. C. Sales, S. McGill, J.-W. Kim, and Z. Islam, Phys. Rev. Lett. **101**, 227602 (2008).
[4]W. Wu, V. Kiryukhin, H. J. Noh, K. T. Ko, J.-H. Park, W. Ratcliff, P. A. Sharma, N. Harrison, Y. J. Choi, Y. Horibe, S. Lee, S. Park, H. T. Yi, C. L. Zhang, and S. W. Cheong, Phys. Rev. Lett. **101**, 137203 (2008).
[5]M. H. Phan, N. A. Frey, M. Angst, J. de Groot, B. C. Sales, D. G. Mandrus, and H. Srikanth, Solid State Commun. **150**, 341 (2010).
[6]X. S. Xu, J. de Groot, Q.-C. Sun, B. C. Sales, D. Mandrus, M. Angst, A. P. Litvinchuk, and J. L. Musfeldt, Phys. Rev. B **82**, 014304 (2010).
[7]P. Ren, Z. Yang, W. G. Zhu, C. H. A. Huan, and L. Wang, J. Appl. Phys. **109**, 074109 (2011).
[8]J. de Groot, T. Mueller, R. A. Rosenberg, D. J. Keavney, Z. Islam, J.-W. Kim, and M. Angst, Phys. Rev. Lett. **108**, 187601 (2012).
[9]D. Niermann, F. Waschkowski, J. de Groot, M. Angst, and J. Hemberger, Phys. Rev. Lett. **109**, 016405 (2012).
[10]A. Ruff, S. Krohns, F. Schrettle, V. Tsurkan, P. Lunkenheimer, and A. Loidl, Eur. Phys. J. B **85**, 290 (2012).
[11]M. A. Subramanian, T. He, J. Chen, N. S. Rogado, T. G. Calvarese, and A. W. Sleight, Adv. Mater. **18**, 1737 (2006).
[12]C. R. Serrao, J. R. Sahu, K. Ramesha, and C. N. R. Rao, J. Appl. Phys. **104**, 016102 (2008).
[13]J. Kim, J. S. Ahn, C. U. Jung, C. S. Kim, and B. W. Lee, J. Appl. Phys. **105**, 07D906 (2009).
[14]J. Kim and B. W. Lee, J. Magn. **15**, 29 (2010).
[15]N. Kimizuka, A. Takenaka, Y. Sasada, and T. Katsura, Solid State Commun. **15**, 1321 (1974).
[16]Y. Yamada, S. Nohdo, and N. Ikeda, J. Phys. Soc. Jpn. **66**, 3733 (1997).
[17]Y. Yamada, K. Kitsuda, S. Nohdo, and N. Ikeda, Phys. Rev. B **62**, 12167 (2000).
[18]Y. Horibe, K. Kishimoto, S. Mori, and N. Ikeda, J. Electron Microsc. **54**, i87 (2005).

[19]H. J. Xiang and M.-H. Whangbo, Phys. Rev. Lett. **98**, 246403 (2007).
[20]J. de Groot, K. Marty, M. D. Lumsden, A. D. Christianson, S. E. Nagler, S. Adiga, W. J. H. Borghols, K. Schmalzl, Z. Yamani, S. R. Bland, R. de Souza, U. Staub, W. Schweika, Y. Su, and M. Angst, Phys. Rev. Lett. **108**, 037206 (2012).
[21]Y. Nakagawa, M. Inazumi, N. Kimizuka, and K. Sirator, J. Phys. Soc. Jpn. **47**, 1369 (1979).
[22]J. Iida, M. Tanaka, H. Kito, and J. Atimitsu, J. Phys. Soc. Jpn. **59**, 4190 (1990).
[23]F. M. F. de Groot, J. C. Fuggle, B. T. Thole, and G. A. Sawatzky, Phys. Rev. B **42**, 5459 (1990).
[24]G. van der Laan and I. W. Kirkman, J. Phys.: Condens. Matter **4**, 4189 (1992).
[25]B. T. Thole, P. Carra, F. Sette, and G. van der Laan, Phys. Rev. Lett. **68**, 1943 (1992).
[26]C. T. Chen, Y. U. Idzerda, H.-J. Lin, N. V. Smith, G. Meigs, E. Chaban, G. H. Ho, E. Pellegrin, and F. Sette, Phys. Rev. Lett. **75**, 152 (1995).
[27]The line shapes of the XMCD spectra, obtained at $T = 220$ and 200 K, were almost the same, but the data at 220 K yielded a better quality than those at 200 K. The line shapes of the XAS data do not change for temperature from room temperature down to $T \sim 170$ K.
[28]J. Iida, M. Tanaka, Y. Nakagawa, S. Funahashi, N. Kimizuka, and S. Takekawa, J. Phys. Soc. Jpn. **62**, 1723 (1993).
[29]K. Yoshii, N. Ikeda, Y. Matsuo, Y. Horibe, and S. Mori, Phys. Rev. B **76**, 024423 (2007).
[30]S. Mukherjee, R. Ranganathan, P. S. Anilkumar, and P. A. Joy, Phys. Rev. B **54**, 9267 (1996).
[31]$M(T)$ data of $ErFe_2O_4$ seem to depend on samples. The present data are similar to those of Ref. 22, while the data of Ref. 12 show the general cluster glass behavior, similarly to that in $R =$ Tm and Lu. So, further experiment and analysis need be done in order to understand the sample-dependent magnetic properties of $ErFe_2O_4$.
[32]A. D. Christianson, M. D. Lumsden, M. Angst, Z. Yamani, W. Tian, R. Jin, E. A. Payzant, S. E. Nagler, B. C. Sales, and D. Mandrus, Phys. Rev. Lett. **100**, 107601 (2008).
[33]K.-T. Ko, H.-J. Noh, J.-Y. Kim, B.-G. Park, J.-H. Park, A. Tanaka, S. B. Kim, C. L. Zhang, and S.-W. Cheong, Phys. Rev. Lett. **103**, 207202 (2009).
[34]K. Kuepper, M. Raekers, C. Taubitz, M. Prinz, C. Derks, M. Neumann, A. V. Postnikov, F. M. F. de Groot, C. Piamonteze, D. Prabhakaran, and S. J. Blundell, Phys. Rev. B **80**, 220409 (2009).
[35]H.-J. Noh, H. Sung, J. Jeong, J. Jeong, S. B. Kim, J.-Y. Kim, J. Y. Kim, and B. K. Cho, Phys. Rev. B **82**, 024423 (2010).
[36]These R $3d$ XAS/XMCD data were obtained by using the third harmonics of the synchrotron radiation. We did not measure Er and Tm $3d_{3/2}$ part of the XAS spectra nor the Lu $3d$ XAS spectrum because of the very low intensity of the radiation at the corresponding energies.
[37]Rare-earth oxides would be better as reference materials. However, we could not find the R $3d$ XMCD spectra of magnetic rare-earth oxides. So we have compared our XMCD data to those of rare-earth metals, which are available in the literature. B. T. Thole, G. van der Laan, J. C. Fuggle, G. A. Sawatzky, R. C. Karnatak, and J.-M. Esteva, Phys. Rev. B **32**, 5107 (1985).
[38]J. K. Lang, Y. Baer, and P. A. Cox, J. Phys. F **11**, 121 (1981).
[39]F. Gerken, A. S. Flodstron, J. Barth, L. I. Johansson, and C. Kunz, Phys. Scr. **32**, 43 (1985).
[40]J.-S. Kang, S. W. Han, J.-G. Park, S. C. Wi, S. S. Lee, G. Kim, H. J. Song, H. J. Shin, W. Jo, and B. I. Min, Phys. Rev. B **71**, 092405 (2005).
[41]J. H. Hwang, D. H. Kim, J.-S. Kang, S. Kolesnik, O. Chmaissem, J. Mais, B. Dabrowski, J. Baik, H. J. Shin, J. Lee, B. Kim, and B. I. Min, Phys. Rev. B **83**, 073103 (2011).
[42]C.-J. Kang and B. I. Min (unpublished).